High Temperature Oxidation Behavior of P91, P92 and E911 Alloy Steels in Dry and Wet Atmospheres

Palanivel Mathiazhagan 1,* and Anand Sawroop Khanna 2

- ¹ Pondicherry Engineering College, Pondicherry, India
- ² Indian Institute of Technology Bombay, Mumbai, India

Abstract. The oxidation behavior has been studied under both dry and wet oxidation atmosphere at 873 K to 1073 K. In dry atmosphere the oxidation resistance of these alloys has been described by the formation of a protective oxide FeCr₂O₄ at 873 K to 973 K. At 1073 K, the kinetics are parabolic with fast growing oxide leading to spalling of oxide for P92 alloy. Oxide scale formed in air was protective with a chromium rich scale at 873–973 K, while double layered oxides were formed at 1073 K with iron oxide an outer layer and inner Cr-rich spinel FeCr₂O₄. In wet atmosphere oxide scale was reasonably different. The oxide layer showed porous in wet atmospheres where as dense oxide layer formed during dry oxidation. The oxidation rate of P92 alloy is about 3, 2 and 1 orders of magnitude higher than the P9, P91 and E911 alloys in wet atmospheres.

Keywords. Oxidation, effect of atmosphere, SEM, XRD, EDAX.

PACS® (2010). 81.65.Mq.

1 Introduction

The thermal efficiency of steam power plant can be improved significantly by increasing the temperature and pressure of the steam entering the turbine inlet from 853 K to 893 K providing a thermal efficiency increase from 38% to 42% [1]. These efficiency gains alone would cut the release of CO₂ and other emission. At such high temperature the commonly used low alloy steels and higher corrosion resistant 12% Cr steels can no longer be used as construction materials for live steam piping because of the lack of creep resistance of these materials. Therefore a number of modified 9%Cr steels such as P91, P92 and E911 were developed to fulfill the new materials requirements in respect to creep strength. These steels exhibit significantly higher creep strength than the conven-

Corresponding author: Palanivel Mathiazhagan, Mechanical Engineering Dept., Pondicherry Engineering College, Pondicherry 605014, india; E-mail: pmathi@pec.edu.

Received: July 17, 2010. Accepted: ???.

tional 2.25 Cr–1Mo and 9Cr–1Mo steels due to small additions of W, Nb and V [2]. It has been shown that, in spite of the high temperatures these steels show adequate oxidation resistance in air [3]. However it was found that oxygen contained wet atmosphere, the oxidation rate of these steels can be several orders of magnitude higher than in air [3]. This detrimental effect of water vapor on the oxidation resistance of FeCr alloys has in fact been known for many years [4,7]. The main objective of this paper to study the oxidation behavior of these alloys in dry and $O_2 + 50 \% H_2O$ atmosphere conditions. Also there will be focus on the microstructure of these alloys in comparison to that of the conventional P9 and P91 alloys.

2 Experimental Procedure

Specimens with a size of $10~\text{mm} \times 10~\text{mm} \times 2~\text{mm}$ thickness were cut from plate. The chemical composition of the steels was determined with inductively coupled and Atomic emission Spectroscopy (ICP-AES) technique and is tabulated in Table 1. For the oxidation studies the specimens were mechanically polished with SiC paper up to a grit number of 800 and ultrasonically cleaned in acetone and dried before the oxidation test.

For dry oxidation test were carried out in horizontal furnace fitted with a (32 mm) diameter Quartz glass tube. All exposures were isothermal; the temperature was kept at 873 K to 1073 K up to 1000 h. It was then isothermally oxidized for a definite period of time, specimen taken out the furnace, cooled to room temperature. Weight changes were noted periodically after definite intervals.

The wet oxidation test samples were mounted in alumina boat which was introduced in horizontal reaction tube and samples were positioned parallel to the direction of gas flow. The furnace was equipped with a PID (Proportional Integral and Derivative) controller to control the desired temperature. The reaction atmosphere of $(O_2 + 50 \% H_2O)$ gas mixture was obtained by bubbling purified O_2 (99.999 % pure) gas through saturator (water flask) containing distilled water. The distilled water temperature was thermostatically controlled at 354 \pm 1 K producing water vapor concentration of 50 %. After exposure, the samples were taken out from the furnace at different intervals, cooled to room temperature and weight changes were measured using a semi-micro balance. The surfaces of the oxide scales were subsequently

alloy	С	Al	Si	P	Nb	Mo	V	Cr	Mn	Ni	W	Fe
P9	0.1	_	0.22	0.025	_	1.1	_	8.5	0.73	0.27	_	Bal
P91	0.1	0.04	0.37	0.01	0.07	0.9	0.2	9.3	0.5	0.23	_	Bal
P92	0.12	0.003	0.04	0.011	0.062	0.5	0.22	8.98	0.47	0.07	1.8	Bal
E911	0.11	0.001	0.1	0.006	0.065	1.1	0.23	8.8	0.33	0.08	1	Bal

Table 1. Chemical composition of the tested steels (mass %).

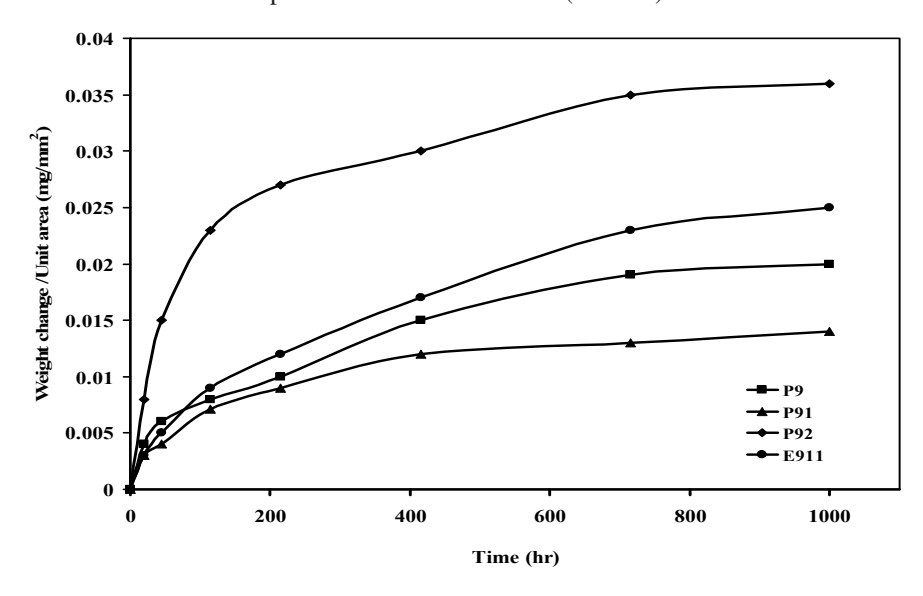


Figure 1. Weight change vs. time plots for the oxidation of alloys at 873 K in air for 1000 h.

examined scanning electron microscopy (SEM) equipped with an EDX analyzer to elucidate the chemical composition. The chemical phases of the scales were determined by X-ray diffraction (XRD) at room temperature.

3 Results and Discussion

3.1 Oxidation Kinetics in Air

The results of long term exposure tests have shown in Figures 1-3. At 873 K, P9, P91 and E911 alloys shows similar weight gain during initial period and increase weight gain with increasing time and follow parabolic behavior. However P92 alloy shows higher weight gain and P91 shows lower weight gain at this temperature. All alloys shows parabolic behavior at 973 K. At 1073 K, kinetics appears to be linear during initial stage for P92 alloy, sudden decrease in weight gain noted around 100 h exposure, due to the spallation of oxide. P9 and P91 alloys showed parabolic behavior with very less weight gain. However E911 alloy shows linear behavior at this temperature. The parabolic rate constants measured by plotting the square of weight gain as a function of time. Parabolic rate constant values are tabulated in Table 2 which indicates that Kp values increases with temperature. The result indicates temperature has a strong influence on oxidation of these alloys. It can therefore be concluded that the oxidation behavior of these alloys strongly depend on the oxidation temperature.

3.2 Oxide Scale Analysis

X-ray diffraction patterns carried out on the oxidized sample of P92 alloy in air at 873 K to 1073 K for 1000 h are shown in Figure 4. The result indicates that the $FeCr_2O_4$, Cr_2O_3 , oxides were formed at 873 and 973 K, however the peak $FeCr_2O_4$ disappeared and strong peak Fe_2O_3 was observed at 1073 K. The oxidation rate of this alloy is higher at 1073 K due to the formation Fe_2O_3 oxide on the surface of the alloy.

3.3 Analysis of Surface Morphology

The results are shown in Figure 5 is the morphology of oxide scales formed on specimens exposed in air at 1073 K for 1000 h. At 1073 K, the sharp crystalline structure was observed (Figure 5(a)) for P9 alloy and this structure is identified from EDAX data to be of Cr₂O₃. The oxides look like nodules with porous and later shows iron rich oxide having rosette appearance with cracks of (Fig 5(b–c)) P91 and P92 alloys, E911 alloy shows crystalline structure with spherical Fe₂O₃ oxide (Fig 5(d)).

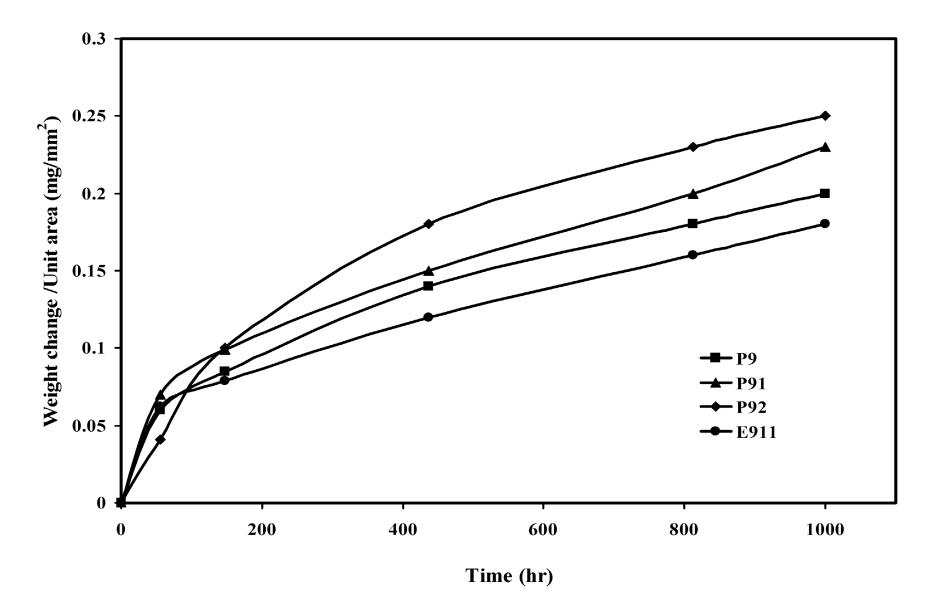


Figure 2. Weight change vs. time plots for the oxidation of alloys at 973 K in air for 1000 h.

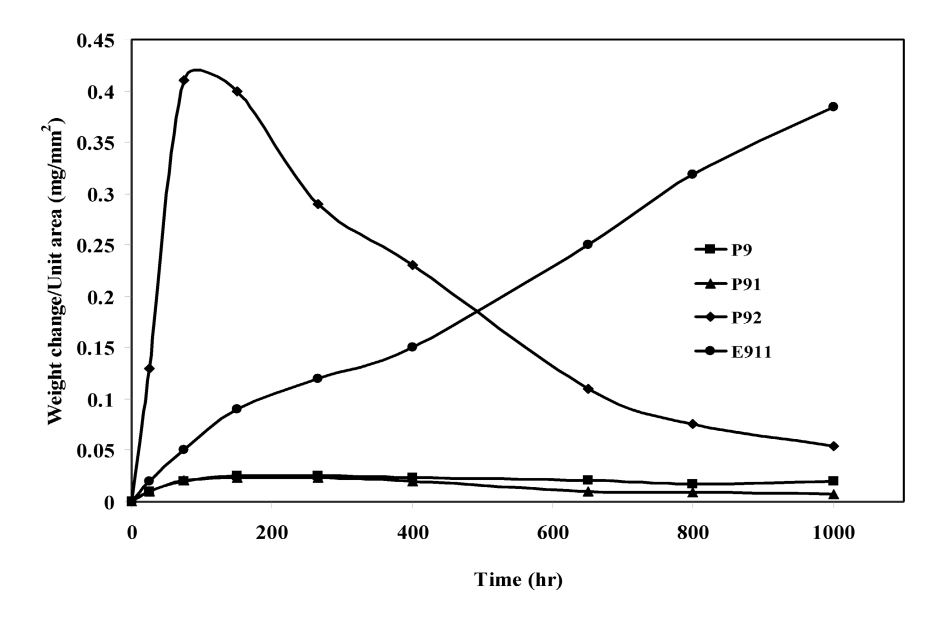


Figure 3. Weight change vs. time plots for the oxidation of alloys at 1073 K in air for 1000 h.

Temperature (K)	Alloy P9	Alloy P91	Alloy P92	Alloy E911
873	$4x10^{-7}$	$2x10^{-7}$	$1x10^{-6}$	$7x10^{-7}$
973	$4x10^{-5}$	$5x10^{-5}$	$6x10^{-5}$	$3x10^{-5}$
1073	0.4×10^{-3}	0.5×10^{-3}	0.8×10^{-3}	0.6×10^{-3}

Table 2. Parabolic rate constants (Kp) in air $(mg^2 mm^{-4} h^{-1})$.

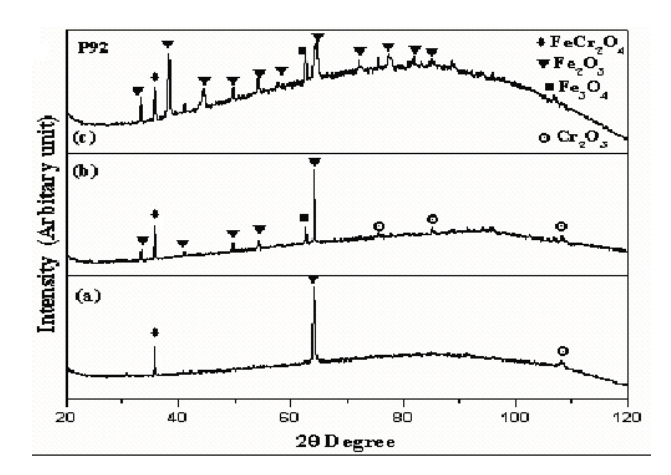


Figure 4. XRD-Pattern of P92 alloy after oxidation in air (a) 873 K (b) 973 K and (c) 1073 K for 1000 h.

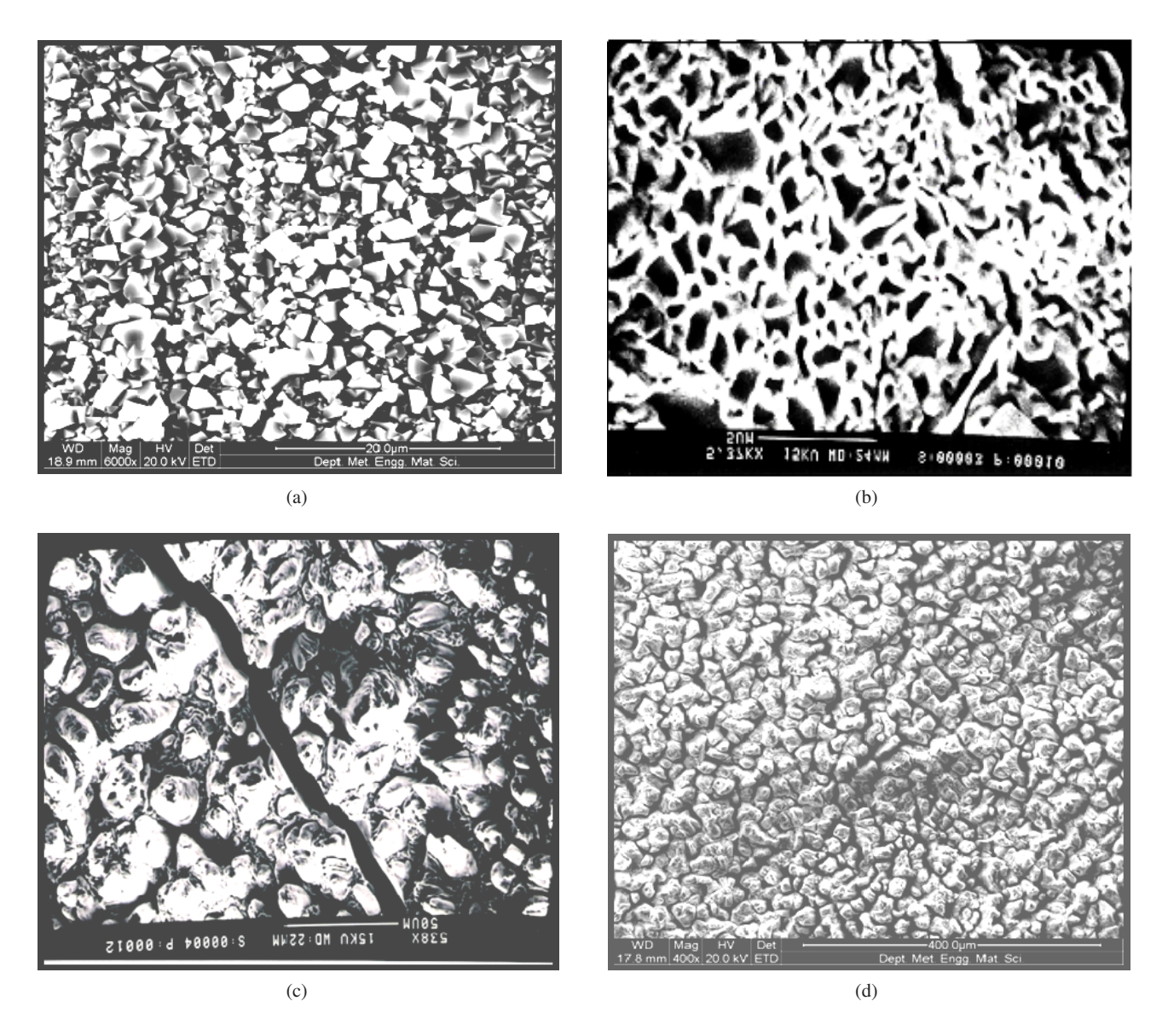


Figure 5. SEM Micrographs of alloys (a), P9, (b) P91, (c) P92 and (d) E911 in air at 1073 for 1000 h.

Alloy	Location	Element (mass %)						
		Si	Nb	Cr	Mn	W	Fe	
P92 1073 K	1	0.81	1.38	15.2	0.37	2.93	79.31	
	2	0.64	2.24	0.33	0.66	_	93.21	

Table 3. EDAX analysis of various points on the oxide scale P92 alloys at 1073 K.

Temperature (K)	Alloy P9	Alloy P91	Alloy P92	Alloy E911
873	1×10^{-6}	5×10^{-6}	2×10^{-6}	8×10^{-7}
973	9×10^{-7}	7×10^{-7}	5×10^{-5}	7×10^{-6}
1073	1×10^{-3}	2×10^{-3}	3×10^{-3}	4×10^{-3}

Table 4. Parabolic rate constants (Kp) of alloys $O_2 + 50 \% H_2O (mg^2 mm^{-4} h^{-1})$.

3.4 Analysis of Cross Section

SEM Micrographs showing the cross sectional view of oxidized P92 alloy at 1073 K in air for 1000 h is shown in Figure 6. Double layer of oxide scales were observed in the alloy. The inner layer very compact with matrix and outer layer contain many voids also separated from inner layer. EDAX analysis was carried out at different location and values are presented in Table 3. The result shows that the presence of chromium rich with small amount of W (2.93 mass %) and Nb (1.38 mass %) oxide along with the major part of Fe-oxide formed on inner layer. However the tungsten (W) and niobium (Nb) having a great affinity for oxygen and form WO₃ oxide. This indicates formation of WO₃at the initial stage of oxidation giving a higher oxidation rate at this stage.

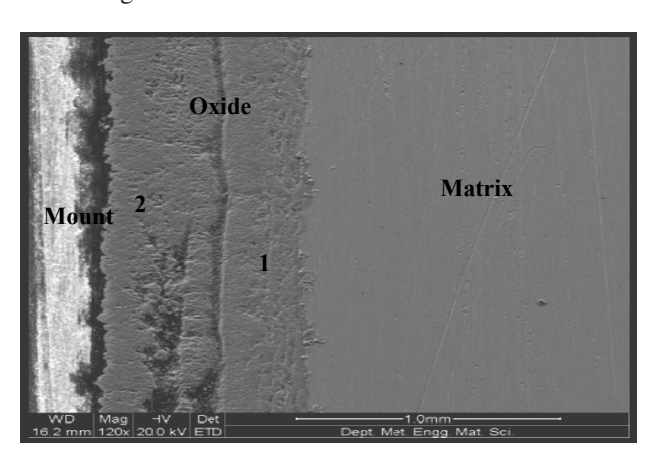


Figure 6. SEM Micrograph of the cross section of P92 alloy oxidized in air at 1073 for 1000 h.

3.5 Oxidation kinetics in $O_2 + 50 \% H_2O$

Weight change vs. time plots for alloy oxidized in O_2 + 50 % H_2O conditions are shown in Figures 7–9. Almost similar weight gain observed for the P9 and E911 alloys;

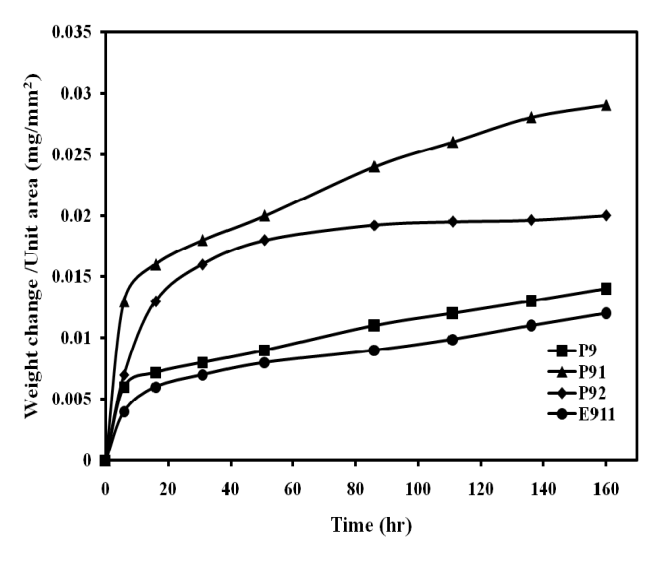


Figure 7. Weight change vs. time plots for alloys oxidized at 873 K in $O_2 + 50 \% H_2O$.

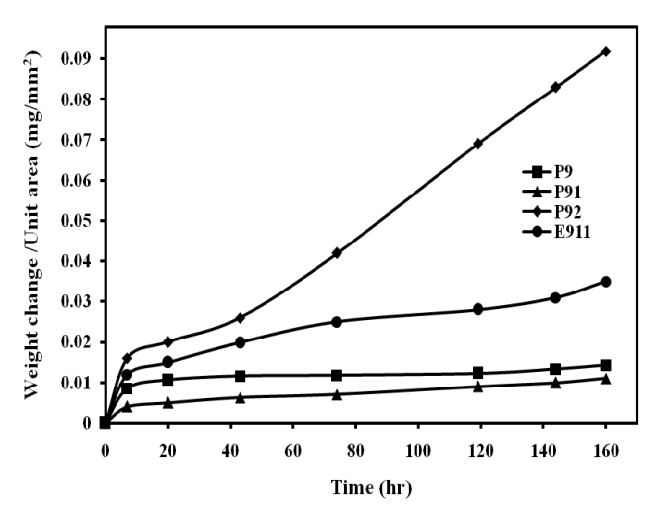


Figure 8. Weight change vs. time plots for alloys oxidized at 973 K in $O_2 + 50 \% H_2O$.

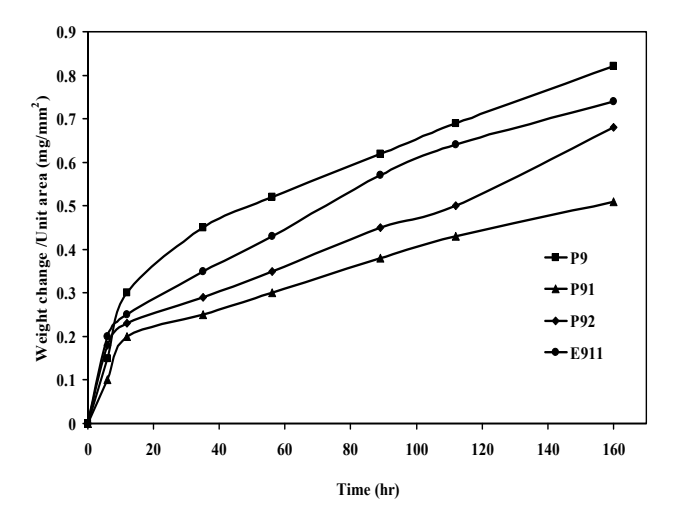


Figure 9. Weight change vs. time plots for alloys oxidized at $1073 \text{ K in O}_2 + 50 \% \text{ H}_2\text{O}$.

however alloy P91 and P92 shows higher weight gain and follows parabolic behavior at 873 K At 973 K, P92 alloy shows a slow initial weight gain occurred up to 40 h and kinetics changed to linear. At 1073 K, P92 alloy shows higher weight gain and P9 shows smaller weight gain, at the initial stage all alloys showed same behavior after that the trend is changed to linear. Parabolic rate constants calculated and presented in the Table 4.

3.6 Oxide Scale Analysis

In order to identify the phases present in the oxidation products, the X-ray diffraction carried out on oxidized P91, E911 and P92 alloys in $O_2 + 50$ % H_2O at 973 K are shown in Figure 10. The result indicates that the dominant peak $FeCr_2O_4$ formed for all alloys followed by weak peaks Cr_2O_3 , Fe_3O_4 and Fe_2O_3 were identified. The sequence of the oxide layers formed also confirms previous observations [6].

3.7 Analysis of Cross Section

SEM/EDAX result of the E911 and P92 alloys are given Figures 11–12. Figure 11 shows that the oxide scales exhibit double layers structure, the inner layer attached to the matrix and outer layer little detached from inner layer for E911 alloy. Small voids are seen to have formed at the oxide metal interface. These could have resulted from condensation of inwardly diffusing cation vacancies at the scale/alloy interface. The inner layer consists a mixture of Cr, W and Fe oxides with little amount of Nb was present in Table 5 at 1073 K. However, P92 alloy the oxide scale is clear and a gap between the outer Fe₂O₃ and the rapidly growing Fe₃O₄ has developed. Further growth depends on the transport processes across the gap proposed by Rahmel and To-

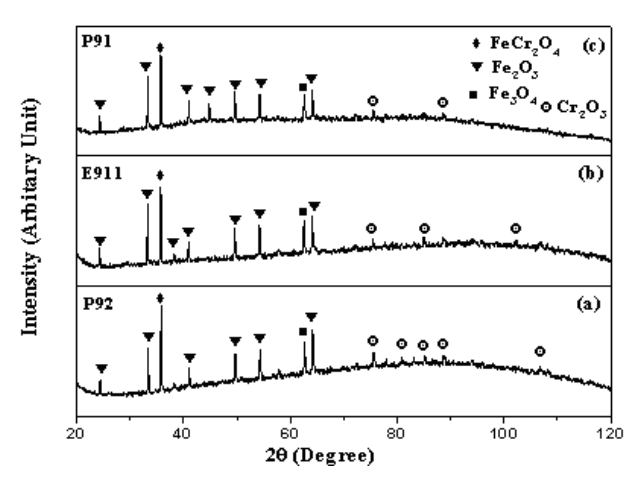


Figure 10. XRD-Pattern of alloys after oxidation in $O_2 +50 \% H_2O$ at 973 K.

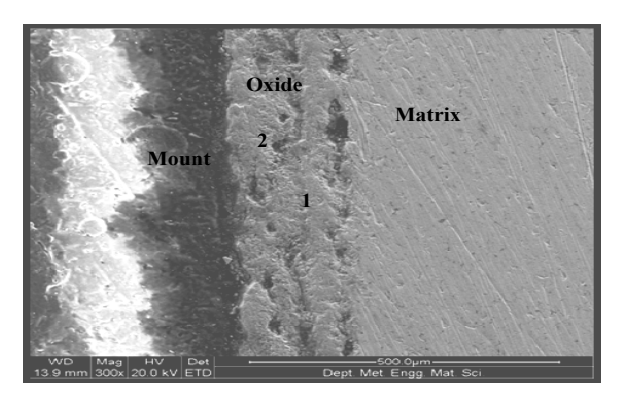


Figure 11. SEM micrograph of the cross section of E911 alloy oxidized at 1073 K.

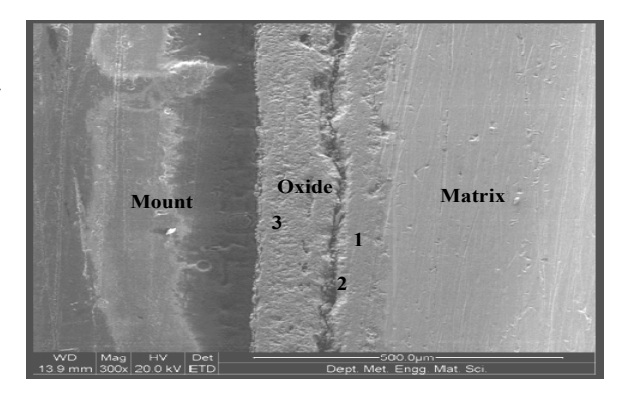


Figure 12. SEM/EDAX micrograph of the cross section of P92 alloy oxidized at 1073 K.

bolski [5] to be by H_2/H_2O bridges. The transport of Fe cations to the gas scale interface becomes increasingly difficult due to the gap, and the resulting decrease in the Fe activity leads to the formation of hematite, the equilibrium phase at the gas scale interface. The same type of oxide scale formed for P92 (Figure 12) alloys in $O_2 + 50 \% H_2O$

Alloy	Location	Element (mass %)						
Alloy	Location	W	Nb	Cr	Mn	Fe		
E911 1073 K	1	4.74	2.36	11.46	1.23	80.21		
L911 10/3 K	2	_	1.41	_	_	98.59		

Table 5. EDAX analysis of various points on E911 alloys at 1073 K.

Alloy	Location	Element (mass %)						
Alloy		W	Cr	Si	Mo	Mn	Fe	
	1	9.54	13.14	_	3.2	2.8	71.32	
P92 1073 K	2	7.96	10.2	_	2.3	2.1	77.44	
	3	_	3.08	_	_	0.93	95.99	

Table 6. EDAX analysis of various points on P92 alloys at 1073 K.

environmental condition. The type of scale is often observed on high Cr steel exposed in Ar containing 5–50 % vol % H_2O [5]. The amount of Fe_2O_3 formed depends on the H_2O content of the atmosphere [8]. Additionally, the EDAX data Table 6 showed that the inner oxide layer containing chromium rich, iron oxide and W also observed, while the most external ones only contain iron and oxygen, thus corresponding to iron oxides.

The allowable metal temperature of these alloys for power plant application generally does not exceed above 873 K, the oxidation experiments carried out in the present study are from 873 to 1073 K. The higher temperature was chosen to obtain measurable changes in weight gain in a reasonable time by accelerating the oxidation process.

In general, the oxidation behavior of these alloys is quite good, most of the alloys showed parabolic behavior and the scale was mainly a mixture of iron and chromium oxide, which protected the alloys from further oxidation. It is interesting to note that the modified alloys such as P92 and E911, which have elements like W, Nb and V shows marginal higher oxidation rate at 1073 K. For example parabolic rate constant of this alloy is 8×10^{-5} mg² mm⁻⁴ h⁻¹ whereas the parabolic rate constant of P9 and P91 is 4×10^{-5} and 5×10^{-5} mg² mm⁻⁴ h⁻¹ in dry condition.

The higher oxidation rate of modified alloy P92 may be due to the presence of active elements such as W, Nb and V in the oxidation process. The presence of W and Nb has been confirmed from EDAX analysis for P92 alloy at 1073 K shown in Figure 6. The concentration of tungsten (W) and niobium (Nb) in the oxide is 2.93 and 1.38 atomic weight percentage (mass %).

The parabolic rate constant (Kp) of P92 alloy is about 3, 2 and 1 orders of magnitude higher than the P9, P91 and E911 alloys in $O_2 + 50 \% H_2O$ environment. Table 7 shows the comparison the oxidation behavior of these alloys at dry and wet environmental condition at 1073 K.

Alloys	Parabolic rate constants (kp) (mg ² mm ⁻⁴ h ⁻¹)				
	$Air \times 10^{-3}$	$O_2 + 50 \% H_2O \times 10^{-3}$			
P9	0.4	1			
P91	0.5	2			
P92	0.8	4			
E911	0.6	3			

Table 7. Parabolic rate constants $(mg^2 mm^{-4} h^{-1})$ at 1073 K.

The higher oxidation rate of P92 alloys obtained in $O_2 + 50\% H_2O$ condition compared to other alloys may be due to high concentration of active element tungsten (W) present in the inner scale (Figure 12). Presence of W is confirmed by EDAX analysis carried out at different location of oxide scale. The concentration of tungsten (W) is 9.54 and 7.96 (atomic weight percentage (mass %)) inner oxide scale. However E911 alloy show that the concentration of active element W and Nb in the oxide is less compared to P92 alloy (Figure 11). This is confirmed with EDAX, the values are 4.74 and 2.36 (mass %)) for W and Nb in the oxide scale. Also confirmed with oxide scale thickness measured values are 150 μ m for E911 alloy (Figure 11) and 214 μ m for P92 alloy (Figure 12). The same types of oxide thickness were obtained in the earlier results [9].

Although, the enhanced oxidation in water vapors is seen by all the low alloy steels studied viz: P9, P91, P92 and E911, however, the enhance oxidation rate of P92 and E911 compared to P9 and P91 can be attributed to the incorporation of tungsten and niobium oxides, simultaneously oxidize along with main alloying elements.

4 Conclusion

The present study has shown that the oxidation of P92 and E911 alloys with the addition of active elements such as W and Nb, which improve the mechanical strength and creep strength of these alloys, is not improved compared to the conventional P9 and P91 alloys. P9 and P91 alloys provide better oxidation resistance at high temperature than the other two alloys.

Higher oxidation rates of P92 and E911 alloy can be attributed to substantial oxidation of active element W. The effect is more pronounced at 1073 K.

Among the four low alloy steels, the oxidation resistance of P92 was observed in the following order as P92 < E911 < P91 < P9 in at 1073 K.

References

[1] P.J. Ennis and W.J. Quadakkers, *International Journal of Pressure vessels and piping*, **84** (2007), 82–87.

- [2] W. J. Quadakkers, J. Ehlers, V. Shemet and L. Singheiser, Proceeding of International Symposium on Materials Ageing and Life Management, October 3–6, Kalpakkam, India (2000).
- [3] J. Ehlers., D. J. Young, E. J. Smaardijk., A. K. Tyagi., H. J. Penkalla, L. Singheiser., W. J. Quadakkers, *Corrosion Science*, 48 (2006), 3428–3454.
- [4] C. T. Fujii and R. A. Meussner, *The Journal of Electrochemical Society*, **110** (12) (1963), 1195–1204.
- [5] A. Rahmel and J. Tobolski, *Corrosion Science*, 5 (1965), 333–346.
- [6] D. Laverde, T. Gomez-Acebo, F. Castro, Corrosion Science, 46 (2004), 613–631.
- [7] A. S. Khanna and P. Kofstad, *Metal Materials Processes*, 1(3), 177–196 (1989).
- [8] B. Tveten, G. Hultquist and T. Norby, Oxidation of metal, 51 (3–4) (1999), 221–233.
- [9] L. Mikkelsen and S. Linderoth, Materials Science and Engineering, A361 (2003), 198–212.